

PAPER • OPEN ACCESS

Acquisition of multiple photon pairs with an EMCCD camera

To cite this article: Eliot Bolduc *et al* 2017 *J. Opt.* **19** 054006

View the [article online](#) for updates and enhancements.

Related content

- [Photon-number correlation for quantum enhanced imaging and sensing](#)
A Meda, E Losero, N Samantaray et al.
- [Biphoton transmission through non-unitary objects](#)
Matthew Reichert, Hugo Defienne, Xiaohang Sun et al.
- [A characterization of the single-photon sensitivity of an electron multiplying CCD](#)
Lijian Zhang, Leonardo Neves, Jeff S Lundeen et al.

Acquisition of multiple photon pairs with an EMCCD camera

Eliot Bolduc, Daniele Faccio and Jonathan Leach

SUPA, School of Engineering and Physical Sciences, Heriot-Watt University, Edinburgh EH14 4AS, United Kingdom

E-mail: j.leach@hw.ac.uk

Received 20 July 2016, revised 1 December 2016

Accepted for publication 9 December 2016

Published 18 April 2017



Abstract

The detection and characterization of quantum states of light plays an important role in quantum science. Traditional methods use single-photon detectors, but these are generally limited to point measurements; consequently, multi-pixel devices are now being utilized in quantum measurements, especially in the field of quantum imaging. Here, we demonstrate the capability of an EMCCD camera to record multiple coincidence events originating from parametric downconversion where the mean photon number per pixel is much greater than unity. The multi-pixel nature of the camera enables us to record correlations ranging from ≈ 1 to 10 000 coincidences per frame. This approach to quantum measurements provide mechanisms for recording quantum signatures for bright correlated photon sources.

Keywords: sub-shot-noise, quantum correlations, EMCCD camera

(Some figures may appear in colour only in the online journal)

1. Introduction

The main goals of modern research in quantum mechanics include the advancement of fundamental physics and harnessing its principles to create state-of-the-art technologies. Cameras with high sensitivity have proven to be very useful tools in both of these areas. In particular, electron multiplying CCD (EMCCD) cameras have been used in recent experiments to show strong Einstein–Podolsky–Rosen type correlations [1, 2], indicating in a direct fashion that quantum physics is non-local [3]. This type of work is also of great interest in the field of quantum communications as the information content of the detected state is one of the largest ever measured in a quantum state of light. Additionally, an intensified CCD camera has been used to perform real-time imaging of entangled modes [4]. Moreover, CCD cameras have been used to perform sub-shot-noise imaging, representing an improvement over standard imaging when low-photon-flux is required [5, 6].

The inherent uncertainty related to Poissonian photon statistics is often called ‘shot noise’ and is fundamentally due to the uncertainty relation between photon number and phase [7]. Traditional monochromatic coherent light sources are characterized by Poissonian statistics, whereby the variance of the number of generated photons in a time window is equal to the mean photon number in that same time window. Sub-shot-noise behavior corresponds to a photon number distribution that has a lower variance than the mean, and this behavior is advantageous in situations where the accuracy on photon number is more important than the accuracy on the phase. Sub-shot-noise behavior has shown to be useful for high precision spectroscopy [8], noise reduction in an interferometer [9] and its application to direct gravitational wave detection [10–13], and, as mentioned above, accurate imaging at low light levels (a few thousands photons per camera exposure) [5, 6, 14]. Importantly, Jedrkiewicz *et al* and Blanchet *et al* performed sub-shot-noise correlation measurements of the difference in the number of conjugate photons in a spontaneous parametric downconversion (SPDC) field in the high average-photon-number regime (about 10 photons per pixel) and the low-gain regime (about 0.15 photons per pixel), respectively [15, 16].



Original content from this work may be used under the terms of the [Creative Commons Attribution 3.0 licence](https://creativecommons.org/licenses/by/3.0/). Any further distribution of this work must maintain attribution to the author(s) and the title of the work, journal citation and DOI.

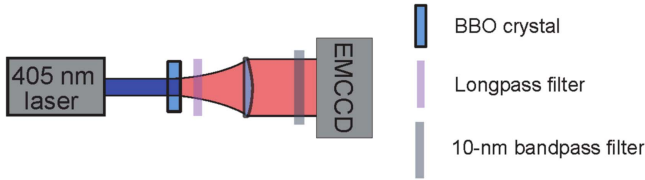


Figure 1. Generating entangled photons via SPDC. Experimental setup used to measure sub-shot-noise correlations. The EMCCD camera is in the far-field of the BBO crystal.

The ability to detect spatial correlations is important for the characterization of sources of spatially entangled photons, and cameras have been widely used to measure spatial correlations in two-photon states generated through SPDC [1, 2, 15, 17–22]. Various studies have shown that efficient CCD cameras allow for the detection of multiple correlated events per frame [15, 17, 19–22].

In this paper, we report coincidence counts ranging from 1 to 10 000 pairs per frame measured with an EMCCD camera, thus making the bridge between the regime of a few events to a large number of events per exposure. We build a model of the number of coincidences detected by the camera as a function of its efficiency and utilize this model to calculate the estimated number of coincidences in a given frame. Moreover, using a calibration independent figure of merit, we report sub-shot-noise photon statistics of the difference between the number of photons in correlated pixels.

2. Theory

2.1. Photon number statistics

The SPDC process works through a nonlinear effect inside a χ^2 crystal, where one pump photon can turn into two photons that are correlated in both the energy and the momentum degrees of freedom. Because of momentum conservation, the two photons of a given pair leave the crystal with opposite transverse momentum, thus arriving at opposite locations of the SPDC ring on the camera (figure 1(a)). We denote these locations by $\mathbf{p} = (x, y)$ and $\mathbf{q} = (-x, -y)$, where x and y are discrete pixel numbers with origins in the center of the SPDC ring. In ideal experimental conditions, the number of photoelectrons n captured by the camera at these locations would be equal. This can be expressed mathematically with $P(k=0) = 1$, where $P(n_p - n_q = k)$ is the probability distribution corresponding to the difference k between the number of photoelectrons detected by the two pixels at locations \mathbf{p} and \mathbf{q} in a given frame. Because of experimental phenomena such as losses and noise in the system, the probability distribution $P(k)$ spreads out, thus increasing its variance $\sigma^2(n_p - n_q)$. Assuming that $\langle n_p - n_q \rangle = 0$, the variance of $P(k)$ can be expressed as $\sigma^2(n_p - n_q) = \langle (n_p - n_q)^2 \rangle$. In two-photon experiments, sub-shot-noise measurements involve a variance $\sigma^2(n_p - n_q)$ that is lower than the mean photon number on the two pixels: $\sigma^2(n_p - n_q) < \langle n_p + n_q \rangle$.

EMCCD cameras are known to introduce a source of error called ‘excess noise’ in the measurement of the number of detected photons in a pixel. This type of noise is due to the stochastic process of multiplying charges and is typically at least equal to the shot noise [23]. One can take this excess noise into account by subtracting its variance from $\sigma^2(n_p - n_q)$ [15]. Although there exists ways to get around the excess noise for a low photon flux (~ 0.15 photon per pixel) [16], excess noise is inevitable in the regime of more than one photon per pixel. As we wish to demonstrate the capabilities of an EMCCD camera in both regimes, we propose the use of a device-independent figure of merit:

$$\kappa = \left\langle \frac{\sigma^2(n_p - n_q)}{\sigma^2(n_p - m_q)} \right\rangle, \quad (1)$$

where $\sigma^2(n_p - m_q)$ is the variance from a shot-noise-limited process measured with the same device. Here, the numbers n_p and m_q are taken at opposite locations \mathbf{p} and \mathbf{q} , respectively, but from independent frames. Finally, the average is done over many frames. Equation (1) is device-independent in that (1) it is independent of the calibration of the camera, and (2) even in the presence of detector noise, a source that is characterized by sub-shot-noise fluctuations will always yield a value that is lower than one, κ (sub-shot-noise) < 1 .

2.2. Coincidence detection

Here we show how to measure coincidence counts with an EMCCD camera. Since EMCCD cameras cannot be gated and do not time tag photon arrival, they cannot directly measure coincidence counts. We thus employ an indirect approach to measure coincidence counts in a pixel pair at locations \mathbf{p} and \mathbf{q} , through the cross-correlation between pixels p and q .

In the supplementary information, we show that the average product of the counts in two correlated pixels is given by

$$\langle n_p n_q \rangle = \eta^2 \langle N^2 \rangle, \quad (2)$$

where η is the detection efficiency of the whole system. Because the photon-pair-generation statistics are Poissonian, the variance of the photon pair number, given by $\langle N^2 \rangle - \langle N \rangle^2$, is equal to the mean photon pair number. We find that the mean number of coincidence counts measured on two correlated pixel can be retrieved through their covariance

$$c = \langle n_p n_q \rangle - \langle n_p \rangle \langle n_q \rangle = \eta^2 \langle N \rangle, \quad (3)$$

where the averages are performed over many frames. We can conclude that the covariance is a measure of the number of coincidences: this result is consistent with the fact that both photons of a pair need to be detected in order to produce a coincidence count, thus leading to the η^2 factor [24]. Crucially, we find that the presence of excess noise does not impact this result. Further, calibrating the camera is necessary to obtain a reliable number of coincidences, and our procedure is detailed in the methods section.

2.3. Experimental setups

We generate entangled photons through the process of parametric downconversion. We pump a 3 mm type-I beta-barium borate (BBO) crystal with a 7 mW 406 nm diode laser (Cobolt). The phase mismatch parameter, which determines the solid angle of the SPDC ring, is set to approximately $\varphi = -4$. We use a low pump power to ensure that we are in the low gain regime, characterized by Poissonian photon statistics. We image the far-field of the exit face of the crystal, where the photons are anti-correlated in their momenta, to the EMCCD camera (Andor iXon 897) using a 100 mm lens. A 10 nm bandpass filter centered at 812 nm is used to block the pump and reduce any ambient light.

3. Results

3.1. Sub-shot-noise correlation measurements

Our experimental procedure is similar to those outlined in references [1, 2, 15, 16]. However, our method for normalization (see methods section) reveal the sub-shot-noise statistics and the coincidence rate even when the mean number of photons per pixel is much greater than unity.

The goal of the experiment is to measure spatial correlations and sub-shot-noise fluctuations for a wide range of mean photon numbers per pixel. The number of photons that is incident on one pixel is controlled by the exposure time of the camera, and we find a linear relationship between these two quantities. The exposure time ranges from 100 μ s to 1 s, spanning a range of coincidences per pixel of about 0.001 to around 100. The full nonlinear relationship between these quantities is shown in the data. At the lower end of this range, the camera is dominated by noise events, and at the upper end of this range some pixels are saturated.

3.2. Sub-shot-noise statistics

The EMCCD camera can detect sub-shot-noise photon statistics over a wide range of exposure times and, by the same token, mean number of photons per pixel (figure 2). We measure the value of κ , the figure of merit for the level of noise relative to the mean photon number, as a function of the camera exposure time (figure 2(a)). Each orange point on the graph corresponds to a value of κ averaged over the illuminated pixels on the ring and over 200 frames, after which the signal rises above the background noise (figure 2(b)). At exposure times lower than 1 ms, background noise and blooming—charge spilling over neighboring pixels—are predominant over the SPDC light, and therefore reduces the strength of the photon number correlations. At exposure times higher than 1 s, the camera is saturated and can no longer detect sub-shot-noise fluctuations accurately.

Figure 3 shows the mean number of coincidences per frame $C = \sum_{x,y} c(x, fy)$ as a function of the mean photon number per pixel $\langle n \rangle = \sum_{x,y} n(x, y) / \sum_{x,y} 1$. For these

calculations, we only sum over the pixels that are illuminated by the downconverted ring.

We see that there is a close to linear relationship between the number of coincidences measured by the camera and the mean photon number per pixel. This results demonstrates the dynamic range of the EMCCD camera in the context of quantum correlation measurements. We see that the camera is able to detect coincidences ranging from 1 to 10 000 per frame, spanning four orders of magnitude. This result is enabled by the large dynamic range of the EMCCD, and thus we are able to take advantage of the fact that the camera can resolve multiple photons arriving at the same pixel, which is in contrast to a single SPAD that only gives a binary outcome. The limitation in the low-photon-number regime is the clock induced charges and the background noise; the limitation in the high-photon-number regime is saturation of the signal on the camera. These limitations shape the nonlinear curve of coincidence number as a function of exposure time from figure 3.

4. Discussion

Our results illustrate the range in which current state-of-the-art EMCCD cameras can be used to measure quantum correlations. Such techniques, where one is able to establish the presence of quantum phenomena, are fundamental to quantum science.

Our method provides a mechanism to detect sub-shot-noise correlations that are present in a source even when a detector adds additional noise. In this sense, while we directly do not record sub-shot-noise correlations in the standard manner, no shot-noise limited source will yield a κ lower than one. We find that the lowest value for κ given the performance of the EMCCD camera is 0.92. As shown in the appendix, the expected value for κ is $1 - \eta/2$, where the factor of 2 comes from the excess noise introduced in the detection process by the gain of the camera. For a SPAD, the factor of 2 is not present and therefore, lower values of κ can be achieved. However, the EMCCD provides the ability to detect the whole SPDC field and spatial correlations, while a SPAD only allows one to measure local correlations. One limiting factor to the quality of our results is the heralding efficiency. The measured heralding efficiency in our experiment is consistent with the efficiencies that have been observed with prior work using similar technology [1]. It is clear that maximizing the heralding efficiency is key to future experiments that use this technology for quantum measurements.

An EMCCD camera is sensitive enough to measure single photons and has a large enough dynamic range to detect more than 100 photons per pixel, as shown in the results section. EMCCD cameras have a larger dynamic range than photon-resolving single pixel detectors, which can resolve 1 to about 25 photons [25–28]. However, these single-pixel detectors are more accurate than EMCCD cameras, which introduce a Poisson-distributed error called ‘excess noise’. Taking the excess noise into account increases the accuracy of the estimation of the coincidence counts detected by the camera.

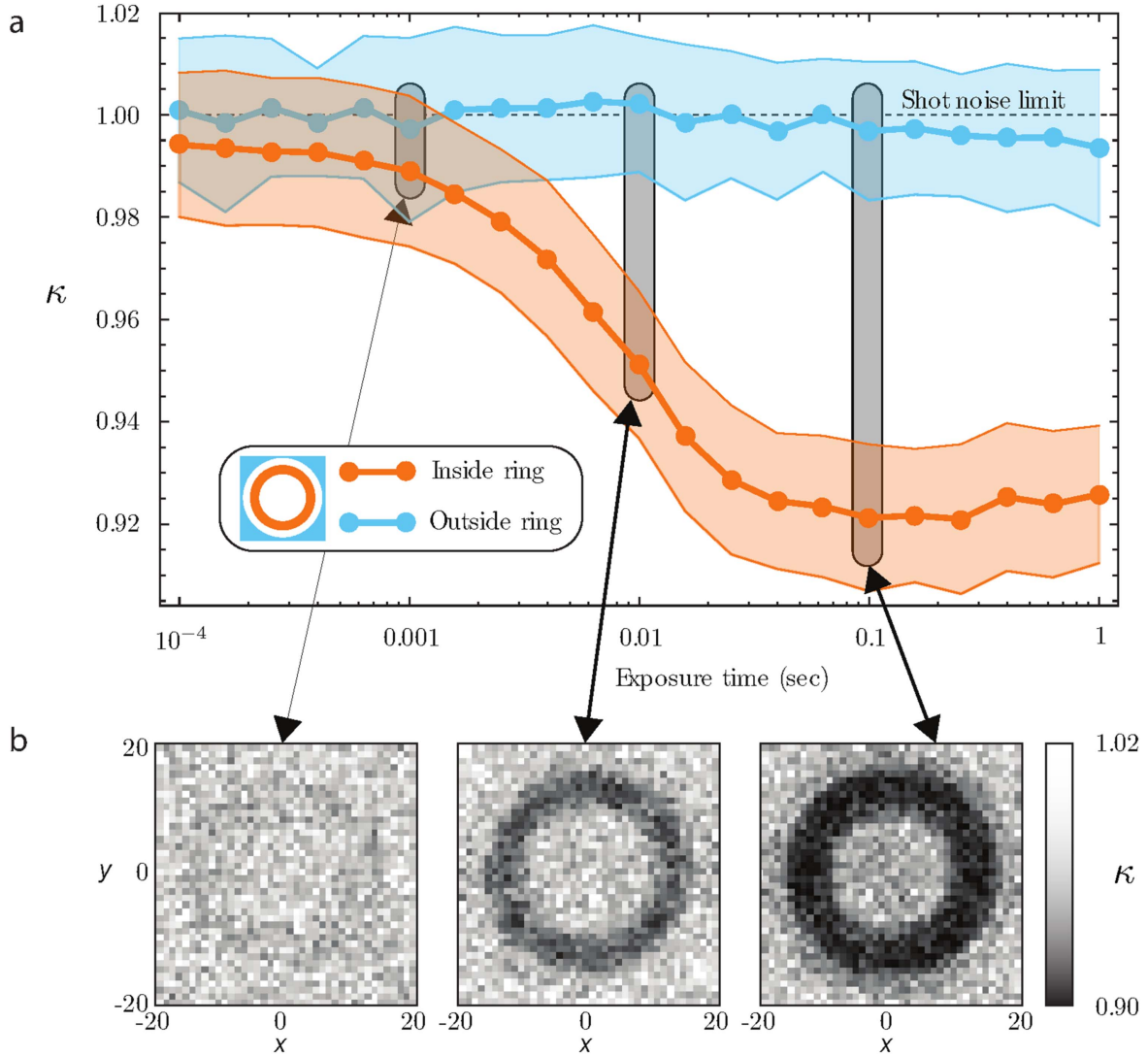


Figure 2. Full-field spatial sub-shot-noise correlations. (a) The shot-noise limit is equal to unity and is indicated on the scale by the dashed black line. The blue curve shows that there are no correlations outside the ring from one frame to the next. The orange line indicates the sub-shot-noise signal inside the ring averaged over 200 frames. The light-colored regions around the solid lines represent the standard deviations on the results. (b) The three bottom images our figure of merit for every pixel for different exposure times. The signal gradually increases with exposure time and makes its way above the background noise.

5. Conclusions

We have demonstrated spatial correlations with an EMCCD camera where the mean photon number per pixel is much greater than one. Taking the excess noise of the camera into account, we provided an analytic method to estimate the number of detected coincidences per frame. We have also shown spatial sub-shot-noise correlations without background subtraction. Our approach allows us to measure photon number correlations for range of input photon number. This new approach to quantum correlation measurements will find uses in applications of quantum imaging and in the measurement of quantum phenomena where multiple photon pairs are generated simultaneously. It will find applications in the characterization of sub-shot noise sources whether they emit a low or high number of photons [29] and application in quantum imaging [5, 30].

Acknowledgments

We acknowledge funding from EPSRC grant numbers EP/M006514/1 and EP/M01326X/1. E B thanks SUPA and the Fonds de recherche Nature et technologies, grant number 176729.

Appendix

Calibration, or lack thereof, of the EMCCD camera. Calibration of a linear camera involves converting electron counts e^- to photon number in the following way $e_{p,q}^- = \alpha n_{p,q} + \beta$, where α and β are parameters that are better found experimentally. The figure of merit κ is not affected by these parameters as they cancel out:

$$\kappa = \frac{\langle (e_p^- - e_q^-)^2 \rangle}{\langle (e_p^- - \varepsilon_q^-)^2 \rangle} = \frac{\langle (n_p - n_q)^2 \rangle}{\langle (n_p - m_q)^2 \rangle}, \quad (4)$$

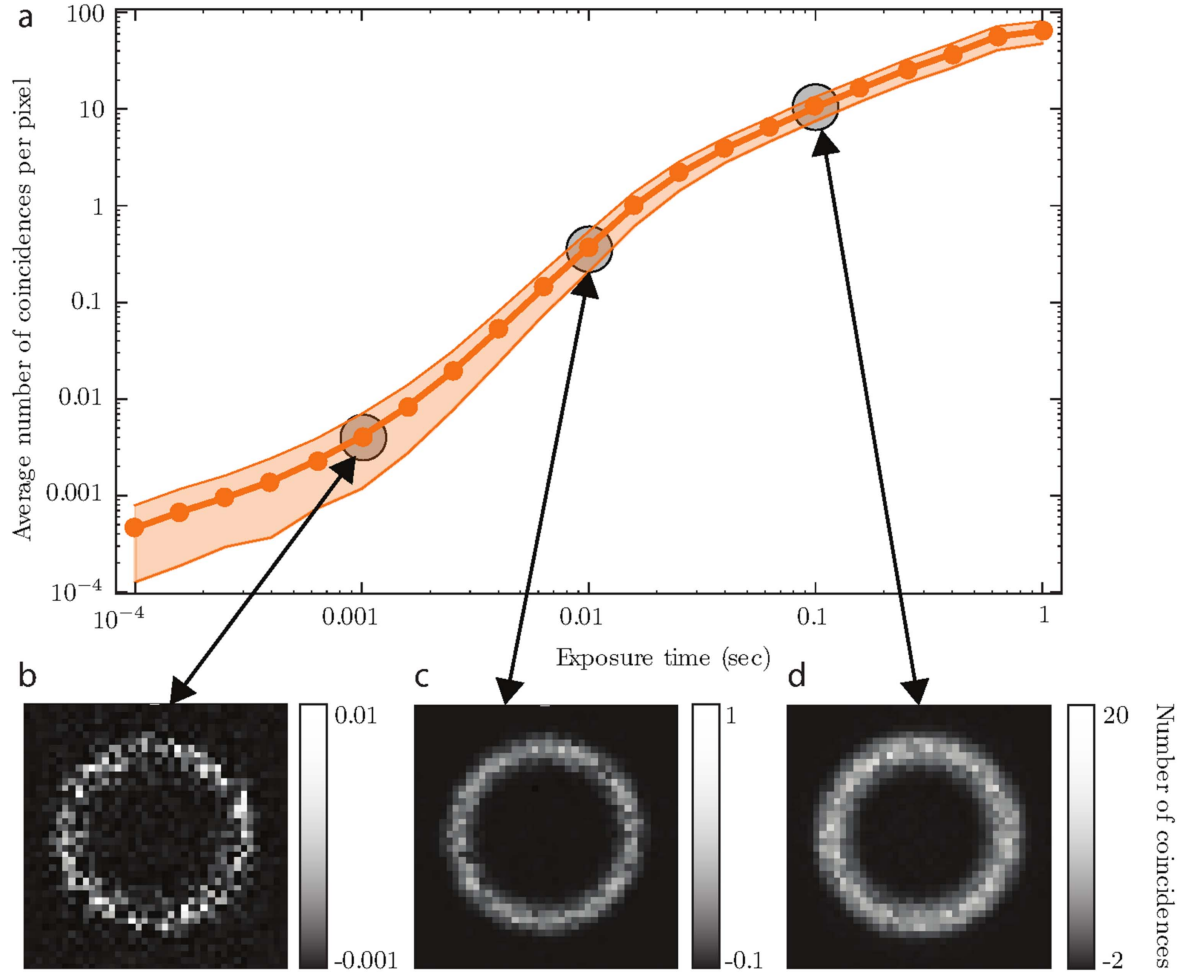


Figure 3. Coincidence data. (a) We sum the number of coincidences over the ring for a given exposure time. At low exposures (< 1 ms), the data are dominated by blooming noise, whereby saturated pixels spill charges onto its neighboring pixels. (b) At an exposure of 1 ms, we see the granularity of the ring image. In these conditions, we detect on the order of one coincidence per frame. (c) The image of the ring gets smoother as the exposure time of the camera is increased to 10 ms. In this regime, the relationship between number of coincidences per frame and exposure time is linear as expected. A two-fold increase in exposure time yields close to a two-fold increase in the number of coincidences per frame. (d) This one-to-one linear relationship disappears at exposure times greater than 100 ms because there is no coincidence signal to be recovered as the ring approaches the limit where it is perfectly smooth: there are no correlated areas on a perfectly smooth surface.

where ε_q represents the electron counts on pixel q from another frame, such that $\varepsilon_q^- = \alpha m_p + \beta$. Further, as shown in the appendix, our model of the losses and the excess noise predicts a value of $\kappa = 1 - \eta/2$, where η is the quantum efficiency of the whole system.

In order to get a correct value of the coincidence rate however, we do need to calibrate the camera accurately. We thus measure the quantum efficiency of the system without the need to calibrate the camera: $\eta = 2(1 - \kappa)$. We then compare this value to the heralding efficiency, which is given by the ratio of the coincidences to the singles. When the camera is calibrated, the heralding efficiency should be equal to the quantum efficiency: $HE = c/s = \eta$. For background subtraction, we simply record the minimum value on the camera and subtract it to the electron counts. For the multiplicative factor, we use the value that equalizes heralding efficiency with quantum efficiency. For all the experiments, the camera gain is set to 1000.

Model of the losses and the excess noise. On one particular pixel pair that we label q and p , we model the statistics

of the source, the losses of the system, the excess noise introduced by the camera and the calibration of the camera. We neglect the clock induced charges as they are always much lower than the singles in our experiment. The following schematic summarizes the model and our notation

$$\text{Source} \xrightarrow[\text{Poisson}]{\text{Pairs}} N \xrightarrow[\text{Binomial}]{\text{Losses}} N_p, \quad N_q \xrightarrow[\text{Poisson}]{\text{Excess noise}} n_p, n_q.$$

As we work in the low-gain SPDC regime, we assume that the photon statistics of the source are given by a Poisson process. Hence, the probability that N photon pairs are incident on pixels q and p is given by

$$P(N) = \frac{\exp(-\langle N \rangle) \langle N \rangle^N}{N!}, \quad (5)$$

where $\langle N \rangle$ is the average number of photons. Out of these N photons incident on pixels p and q , only N_p and N_q are detected. We model losses with a binomial distribution. The

probability that N_p photons are detected given that N pairs were generated is given by

$$P(N_p|N) = \frac{N!}{N_p!(N - N_p)!} \eta^{N_p} (1 - \eta)^{(N - N_p)}. \quad (6)$$

Further, given that N_p photons were detected on pixel x , the excess noise introduces a Poisson-type error, such that the probability that the camera reads out n_p photons given that N_p are detected after losses is given by

$$P(n_p|N_p) = \frac{\exp(-N_p) N_p^{n_p}}{n_p!}. \quad (7)$$

Equivalently, the probabilities corresponding to the number of photons n_q the camera reads out at pixel q are given by equations (6) and (7) where we replace the subscript p by q on every parameter.

We now have the tools to expand $P(n_q, n_p)$ with the conditional probability corresponding to the above physical processes:

$$P(n_p, n_q) = \sum_{N_p, N_q, N} P(n_p, n_q|N_p, N_q) P(N_p, N_q|N) P(N), \quad (8)$$

where all sums are performed from 0 to ∞ , and $P(N_p, N_q|N) = 0$ when $N < \max(N_p, N_q)$. Since the processes are independent at different pixels, we write $P(n_p, n_q|N_p, N_q) = P(n_p|N_p)P(n_q|N_q)$ and $P(N_p, N_q|N) = P(N_p|N)P(N_q|N)$. We also change the order of the sums to simplify the calculation of equation (10)

$$\begin{aligned} \sigma^2(n_p - n_q) &= \sum_N P(N) \sum_{N_p, N_q} P(N_p|N) P(N_q|N) \\ &\quad \times \sum_{n_p, n_q} P(n_p|N_p) P(n_q|N_q) (n_p - n_q)^2. \end{aligned} \quad (9)$$

The result of the sum on (n_p, n_q) is $(N_p + N_q) + (N_p - N_q)^2$. We evaluate the second sum on (N_p, N_q) and find $2N\eta(2 - \eta)$. We finally find $\sigma^2(n_p - n_q) = 2\langle N \rangle \eta(2 - \eta)$. Since the average photon counts is $\eta\langle N \rangle$, the value of the variance is can never be lower than the shot-noise-limit:

$$\sigma^2(n_p - n_q) > \langle n_p + n_q \rangle. \quad (10)$$

It is thus not possible to observe sub-shot-noise behavior with an EMCCD camera without subtracting the variance due to the excess noise, except at very low light levels where excess noise can be suppressed through thresholding [16].

Sub-shot-noise figure of merit. Our figure of merit κ compares the variance $\sigma(n_p - n_q)$ of two correlated pixels to the variance $\sigma(n_q - m_q)$ of two uncorrelated pixels. To calculate $\sigma^2(n_p - m_q)$, we attribute a different number of generated pairs (N and M) to the two different frames. In a similar demonstration to the one for σ^2 , we prove that the shot-noise-limited variance is given by

$$\begin{aligned} \sigma^2(n_p - m_q) &= \sum_N P(N) \sum_M P(M) \sum_{N_p, M_q} P(N_p|N) P(M_q|M) \\ &\quad \times \sum_{n_p, m_q} P(n_p|N_p) P(m_q|M_q) (n_p - m_q)^2. \end{aligned} \quad (11)$$

We find $\sigma^2(n_p - m_q) = 4\langle N \rangle \eta$. In the case of a Poissonian two-photon source measured with an EMCCD camera, our

figure of merit κ thus yields

$$\kappa = \frac{\sigma^2(n_p - n_q)}{\sigma^2(n_p - m_q)} = 1 - \frac{\eta}{2}, \quad (12)$$

where η is due to losses and the factor of 2 is attributed to the excess noise.

Average number of double coincidences. Equation (2) of the main text can be demonstrated by replacing $(n_p - n_q)^2$ by $n_p n_q$ in the rhs of equation (9).

References

- [1] Edgar M P, Tasca D S, Izdebski F, Warburton R E, Leach J, Agnew M, Buller G S, Boyd R W and Padgett M J 2012 Imaging high-dimensional spatial entanglement with a camera *Nat. Commun.* **3** 984
- [2] Moreau P-A, Mougins-Sisini J, Devaux F and Lantz E 2012 Realization of the purely spatial Einstein–Podolsky–Rosen paradox in full-field images of spontaneous parametric down-conversion *Phys. Rev. A* **86** 010101
- [3] Einstein A, Podolsky B and Rosen N 1935 Can quantum-mechanical description of physical reality be considered complete? *Phys. Rev. A* **47** 777–80
- [4] Fickler R, Krenn M, Lapkiewicz R, Ramelow S and Zeilinger A 2013 Real-time imaging of quantum entanglement *Sci. Rep.* **3** 1914
- [5] Brida G, Genovese M and Berchera I R 2010 Experimental realization of sub-shot-noise quantum imaging *Nat. Commun.* **4** 227–30
- [6] Taylor M A, Janousek J, Daria V, Knittel J, Hage B, Bachor H-A and Bowen W P 2013 Biological measurement beyond the quantum limit *Nat. Commun.* **7** 229–33
- [7] Barnett S M and Pegg D T 1989 On the Hermitian optical phase operator *J. Mod. Opt.* **36** 7–19
- [8] Ribeiro P H, Schwob C, Maître A and Fabre C 1997 Sub-shot-noise high-sensitivity spectroscopy with optical parametric oscillator twin beams *Opt. Lett.* **22** 1893–5
- [9] Caves C M 1981 Quantum-mechanical noise in an interferometer *Phys. Rev. D* **23** 1693
- [10] Gea-Banacloche J and Leuchs G 1987 Squeezed states for interferometric gravitational-wave detectors *J. Mod. Opt.* **34** 793–811
- [11] McKenzie K, Shaddock D A, McClelland D E, Buchler B C and Lam P K 2002 Experimental demonstration of a squeezing-enhanced power-recycled Michelson interferometer for gravitational wave detection *Phys. Rev. Lett.* **88** 231102
- [12] Goda K, Miyakawa O, Mikhailov E E, Saraf S, Adhikari R, McKenzie K, Ward R, Vass S, Weinstein A J and Mavalvala N 2008 A quantum-enhanced prototype gravitational-wave detector *Nat. Phys.* **4** 472–6
- [13] LIGO Scientific Collaboration 2011 A gravitational wave observatory operating beyond the quantum shot-noise limit *Nat. Phys.* **7** 962–5
- [14] Kolobov M I and Kumar P 1993 Sub-shot-noise microscopy: imaging of faint phase objects with squeezed light *Opt. Lett.* **18** 849–51
- [15] Jedrkiewicz O, Jiang Y-K, Brambilla E, Gatti A, Bache M, Lugiato L A and Di Trapani P 2004 Detection of sub-shot-noise spatial correlation in high-gain parametric down conversion *Phys. Rev. Lett.* **93** 243601
- [16] Blanchet J-L *et al* 2008 Measurement of sub-shot-noise correlations of spatial fluctuations in the photon-counting regime *Phys. Rev. Lett.* **101** 233604

- [17] Jost B, Sergienko A, Abouraddy A, Saleh B and Teich M 1998 Spatial correlations of spontaneously down-converted photon pairs detected with a single-photon-sensitive CCD camera *Opt. Express* **3** 81–8
- [18] Oemrawsingh S S R, Van Drunen W J, Eliel E R and Woerdman J P 2002 Two-dimensional wave-vector correlations in spontaneous parametric downconversion explored with an intensified CCD camera *J. Opt. Soc. Am. B* **19** 2391–5
- [19] Brambilla E, Gatti A, Bache M and Lugiato L A 2004 Simultaneous near-field and far-field spatial quantum correlations in the high-gain regime of parametric down-conversion *Phys. Rev. A* **69** 023802
- [20] Lugiato L A, Gatti A and Brambilla E 2002 Quantum imaging *J. Opt. B: Quantum Semiclass Opt.* **4** S176
- [21] Mosset A, Devaux F, Fanjoux G and Lantz E 2004 Direct experimental characterization of the Bose–Einstein distribution of spatial fluctuations of spontaneous parametric down-conversion *Eur. Phys. J. D* **28** 447–51
- [22] Brambilla E, Caspani L, Jedrkiewicz O, Lugiato L A and Gatti A 2008 High-sensitivity imaging with multi-mode twin beams *Phys. Rev. A* **77** 053807
- [23] Hyneczek J and Nishiwaki T 2003 Excess noise and other important characteristics of low light level imaging using charge multiplying CCDs *IEEE Trans. Electron Devices* **50** 239–45
- [24] Leach J, Bolduc E, Gauthier D J and Boyd R W 2012 Secure information capacity of photons entangled in many dimensions *Phys. Rev. A* **85** 060304
- [25] Rosenberg D, Lita A E, Miller A J and Nam S W 2005 Noise-free high-efficiency photon-number-resolving detectors *Phys. Rev. A* **71** 061803
- [26] Schuster D I *et al* 2007 Resolving photon number states in a superconducting circuit *Nat. Comm.* **445** 515–8
- [27] Achilles D, Silberhorn C, Sliwa C, Banaszek K, Walmsley I A, Fitch M J, Jacobs B C, Pittman T B and Franson J D 2004 Photon-number-resolving detection using time-multiplexing *J. Mod. Opt.* **51** 1499–515
- [28] Becerra F E, Fan J and Migdall A 2015 Photon number resolution enables quantum receiver for realistic coherent optical communications *Nat. Comm.* **9** 48–53
- [29] Iskhakov T S, Usenko V C, Andersen U L, Filip R, Chekhova M V and Leuchs G 2016 Heralded source of bright multi-mode mesoscopic sub-Poissonian light *Opt. Lett.* **41** 2149–52
- [30] Morris P A, Aspden R S, Bell J E, Boyd R W and Padgett M J 2015 Imaging with a small number of photons *Nat. Commun.* **6** 5913